

**Exposé de soutenance pour le titre de
Docteur de l'École Polytechnique**

Spécialité: Physique

***Ab initio* study of plasmons and
electron-phonon coupling in bismuth:
from free-carrier absorption towards a new
method for electron energy-loss spectroscopy**

Iurii Timrov

27 March 2013, École Polytechnique



Outline

1. Introduction

1.1 Motivation

1.2 Material: Bismuth

1.3 State of the art methods

2. Results

2.1 High-energy response: new approach for EELS

2.2 Low-energy response: free-carrier response

3. Conclusions

Outline

1. Introduction

1.1 Motivation

1.2 Material: Bismuth

1.3 State of the art methods

2. Results

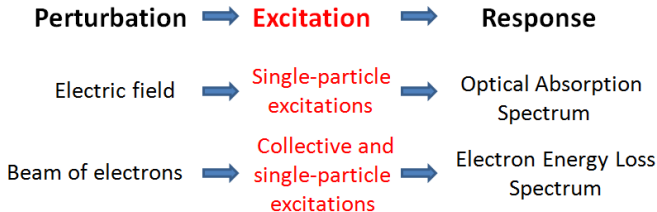
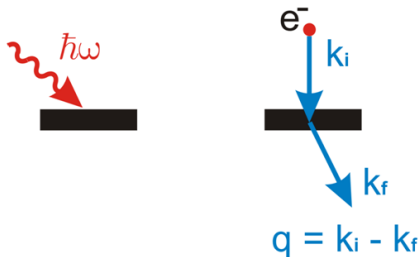
2.1 High-energy response: new approach for EELS

2.2 Low-energy response: free-carrier response

3. Conclusions

Motivation

How to understand the nature of materials?
Perturb them and see what happens!



Motivation

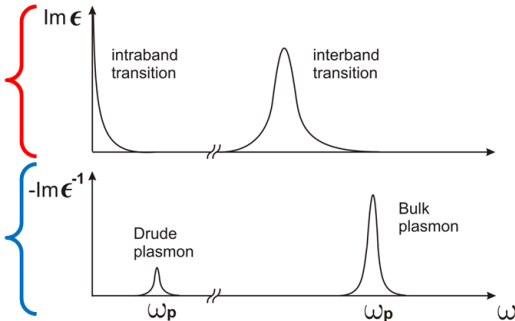
Low-energy
response

High-energy response

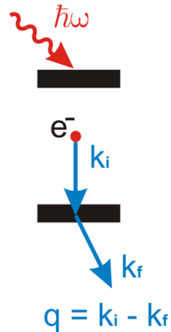
10 - 300 meV

0.3 - 100 eV

Optical
Absorption
Spectrum



Electron
Energy Loss
Spectrum
(EELS)



Optics: $\mathbf{q} \rightarrow 0, \omega \rightarrow 0$

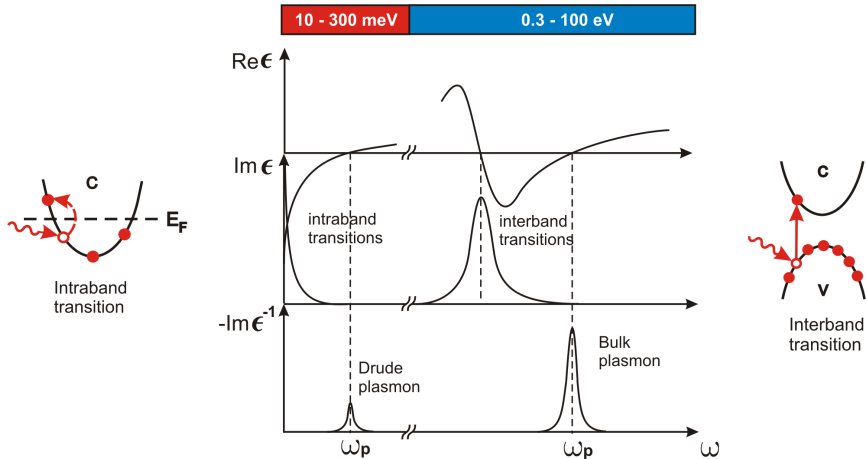
EELS: $\mathbf{q} \neq 0, \omega \neq 0$

Drude model: $\epsilon(\omega) = 1 - \frac{\omega_p^2}{\omega(\omega + i\gamma)}$

Loss function $-\text{Im}[\epsilon^{-1}(\mathbf{q}, \omega)]$

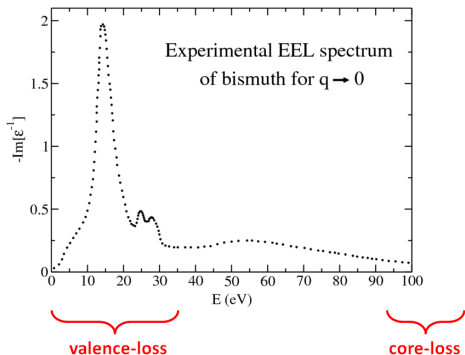
Motivation

Ab initio description of the **full** charge-carrier response of bismuth to external perturbations: **low-energy** and **high-energy** response.



Why do we need a new method for EELS?

1. Bridging the valence-loss and the core-loss EELS.



It is computationally expensive for state-of-the-art methods to describe EEL spectra of complex systems in the energy range up to 100 eV.

C. Wehenkel et al., *Solid State Comm.* **15**, 555 (1974)

Why do we need a new method for EELS?

2. Calculation of EEL spectra of large systems (hundreds of atoms).

Example: Calculation of surface plasmons
⇒ Simulation of the surface is needed

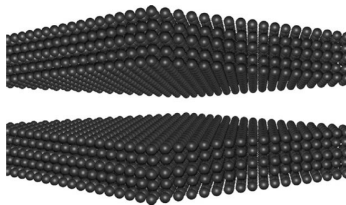


Figure: View of a 5-layer slab model of a surface, as used in periodic calculation.



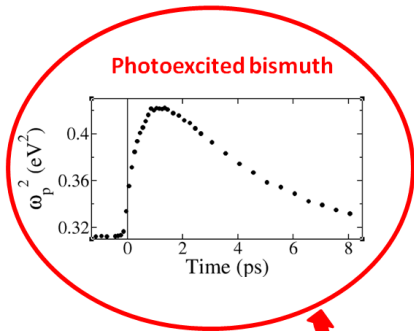
Large number of atoms



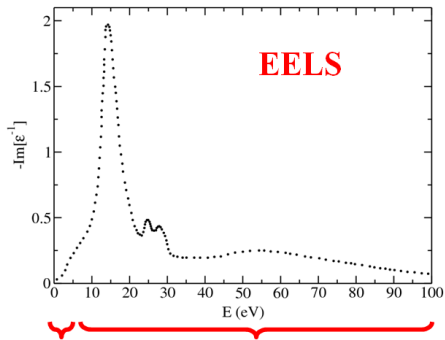
Computationally demanding task for state-of-the-art methods

D. Scholl and J. Steckel, "DFT: A practical introduction" (2009).

Low-energy response: photoexcited bismuth



Low-energy response
(from tens to hundreds of meV)



High-energy response

Photoexcitation of Bi \iff Pump-probe THz expt. (L. Perfetti, J. Faure.)

Theoretical model is needed in order to explain the evolution of the Drude plasma frequency ω_p after the photoexcitation of Bi.

Outline

1. Introduction

1.1 Motivation

1.2 Material: Bismuth

1.3 State of the art methods

2. Results

2.1 High-energy response: new approach for EELS

2.2 Low-energy response: free-carrier response

3. Conclusions

Material: Semimetal Bismuth

SPIN-ORBIT COUPLING

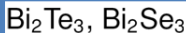
$$\mathbf{L} \cdot \boldsymbol{\sigma}$$

THERMOELECTRICITY

$$ZT = \frac{\rho S^2}{\kappa} T$$



BISMUTH
COMPOUNDS



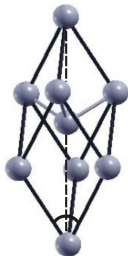
BISMUTH IS
SEMIMETAL AS
GRAPHITE

J.-P. Issi, Aus. J. Phys. **32**, 585 (1979)

M. Z. Hasan and C. L. Kane, Rev. Mod. Phys. **82**, 3045 (2010).

Crystal and Electronic Structure

A7 rhombohedral structure:
Peierls distortion of sc lattice



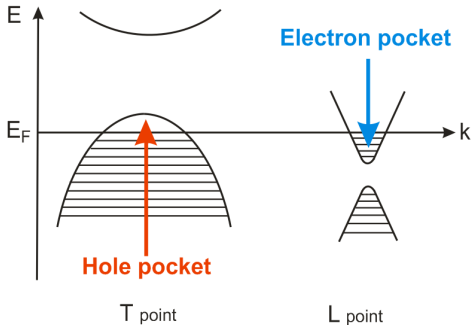
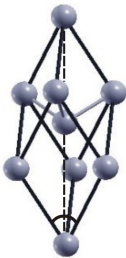
Semimetallicity is due to the Peierls distortion: Overlap between valence and conduction bands.

The Fermi surface consists of **1 hole pocket** and **3 electron pockets**.

Y. Liu et al., Phys. Rev. B **52**, 1566 (1995).
J.-P. Issi, Aus. J. Phys. **32**, 585 (1979)

Crystal and Electronic Structure

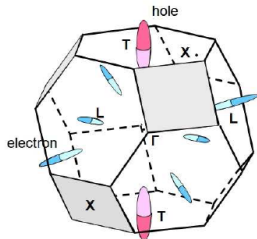
A7 rhombohedral structure:
Peierls distortion of sc lattice



Semimetallicity is due to the Peierls distortion: Overlap between valence and conduction bands.

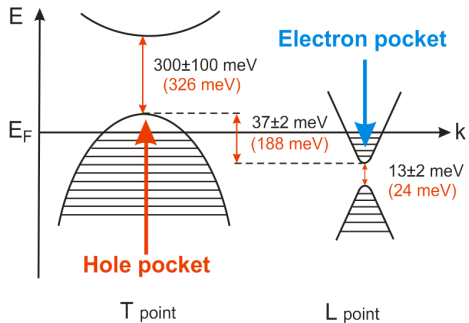
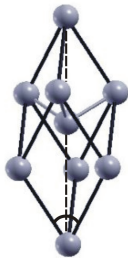
The Fermi surface consists of **1 hole pocket** and **3 electron pockets**.

Y. Liu et al., Phys. Rev. B **52**, 1566 (1995).
J.-P. Issi, Aus. J. Phys. **32**, 585 (1979)



Crystal and Electronic Structure

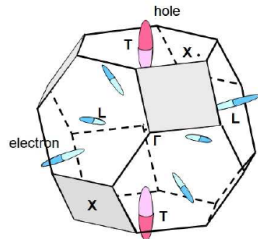
A7 rhombohedral structure:
Peierls distortion of sc lattice



Semimetallicity is due to the Peierls distortion: Overlap between valence and conduction bands.

The Fermi surface consists of 1 hole pocket and 3 electron pockets.

Y. Liu *et al.*, *Phys. Rev. B* **52**, 1566 (1995).
J.-P. Issi, *Aus. J. Phys.* **32**, 585 (1979)



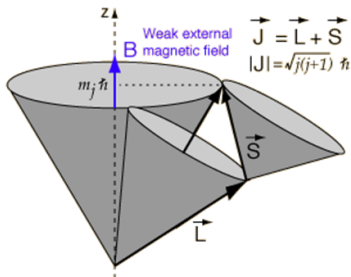
Spin-orbit coupling (SOC)

Spin-orbit coupling is a coupling of electron's spin \mathbf{S} with its orbital motion \mathbf{L} .

The SOC Hamiltonian reads:

$$H_{\text{SOC}} \propto \nabla V (\mathbf{L} \cdot \boldsymbol{\sigma}),$$

where V is the potential, and $\boldsymbol{\sigma}$ are Pauli spin-matrices: $\mathbf{S} = \frac{\hbar}{2} \begin{pmatrix} \boldsymbol{\sigma} & 0 \\ 0 & \boldsymbol{\sigma} \end{pmatrix}$.



material	SOC-assisted splitting of levels at Γ (eV)
Si	0.04
GaAs	0.3
InSb	0.8
As	0.3
Sb	0.6
Pb	1.0
Bi	1.5

In bismuth the spin-orbit coupling is very strong!

A. Dal Corso, *J. Phys. Condens. Matter* **20**, 445202 (2008).

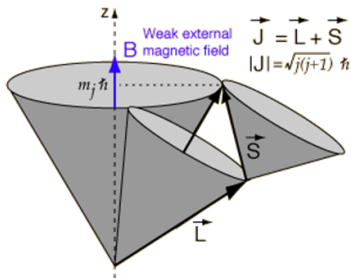
Spin-orbit coupling (SOC)

Spin-orbit coupling is a coupling of electron's spin \mathbf{S} with its orbital motion \mathbf{L} .

The SOC Hamiltonian reads:

$$H_{\text{SOC}} \propto \nabla V (\mathbf{L} \cdot \boldsymbol{\sigma}),$$

where V is the potential, and $\boldsymbol{\sigma}$ are Pauli spin-matrices: $\mathbf{S} = \frac{\hbar}{2} \begin{pmatrix} \boldsymbol{\sigma} & 0 \\ 0 & \boldsymbol{\sigma} \end{pmatrix}$.

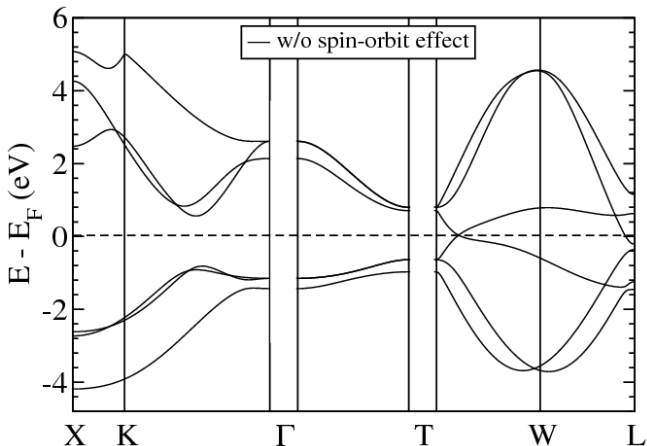


material	SOC-assisted splitting of levels at Γ (eV)
Si	0.04
GaAs	0.3
InSb	0.8
As	0.3
Sb	0.6
Pb	1.0
Bi	1.5

In bismuth the spin-orbit coupling is very strong!

A. Dal Corso, *J. Phys. Condens. Matter* **20**, 445202 (2008).

Kohn-Sham band structure of bismuth

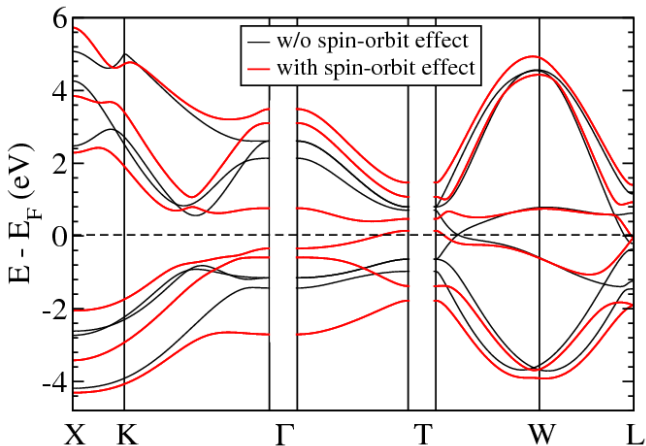


X. Gonze et al., *Phys. Rev. B* **41**, 11827 (1990)

A. B. Shick et al., *Phys. Rev. B* **60**, 15484 (1999)

I. Timrov, J. Faure, N. Vast, L. Perfetti et al., *Phys. Rev. B* **85**, 155139 (2012)

Kohn-Sham band structure of bismuth



X. Gonze et al., *Phys. Rev. B* **41**, 11827 (1990)

A. B. Shick et al., *Phys. Rev. B* **60**, 15484 (1999)

I. Timrov, J. Faure, N. Vast, L. Perfetti et al., *Phys. Rev. B* **85**, 155139 (2012)

Outline

1. Introduction

1.1 Motivation

1.2 Material: Bismuth

1.3 State of the art methods

2. Results

2.1 High-energy response: new approach for EELS

2.2 Low-energy response: free-carrier response

3. Conclusions

Density Functional Theory

Ground-state: DFT

The Kohn-Sham equation:

$$\left(-\frac{1}{2}\nabla^2 + V_{KS}(\mathbf{r})\right) \varphi_i(\mathbf{r}) = \varepsilon_i \varphi_i(\mathbf{r}).$$

The Kohn-Sham potential $V_{KS}(\mathbf{r})$:

$$\int \frac{\rho(\mathbf{r}')}{|\mathbf{r} - \mathbf{r}'|} d\mathbf{r}' + \frac{\delta E_{xc}[\rho(\mathbf{r})]}{\delta \rho(\mathbf{r})} + V_{\text{ext}}(\mathbf{r}).$$

The charge-density:

$$\rho(\mathbf{r}) = \sum_i^{\text{occ}} |\varphi_i(\mathbf{r})|^2.$$

The quantum Liouville equation:

$$[\hat{H}_{KS}, \hat{\rho}] = 0.$$

Hohenberg and Kohn, *Phys. Rev.* (1964)

Kohn and Sham, *Phys. Rev.* (1965)

Historical note



Joseph Liouville

1809 - 1882

Alma mater: École Polytechnique

1827: Graduated from the
École Polytechnique

1838: Appointed as professor at
École Polytechnique

Time-Dependent Density Functional Theory

Ground-state: DFT

The Kohn-Sham equation:

$$\left(-\frac{1}{2}\nabla^2 + V_{KS}(\mathbf{r})\right) \varphi_i(\mathbf{r}) = \varepsilon_i \varphi_i(\mathbf{r}).$$

The Kohn-Sham potential $V_{KS}(\mathbf{r})$:

$$\int \frac{\rho(\mathbf{r}')}{|\mathbf{r}-\mathbf{r}'|} d\mathbf{r}' + \frac{\delta E_{xc}[\rho(\mathbf{r})]}{\delta \rho(\mathbf{r})} + V_{ext}(\mathbf{r}).$$

The charge-density:

$$\rho(\mathbf{r}) = \sum_i^{occ} |\varphi_i(\mathbf{r})|^2.$$

The quantum Liouville equation:

$$[\hat{H}_{KS}, \hat{\rho}] = 0.$$

Hohenberg and Kohn, *Phys. Rev.* (1964)

Kohn and Sham, *Phys. Rev.* (1965)

Excited-state: TDDFT

The TD Kohn-Sham equation:

$$\left(-\frac{1}{2}\nabla^2 + V_{KS}(\mathbf{r}, t)\right) \varphi_i(\mathbf{r}, t) = i \frac{\partial}{\partial t} \varphi_i(\mathbf{r}, t).$$

The TD Kohn-Sham potential $V_{KS}(\mathbf{r}, t)$:

$$\int \frac{\rho(\mathbf{r}', t)}{|\mathbf{r}-\mathbf{r}'|} d\mathbf{r}' + \frac{\delta E_{xc}[\rho(\mathbf{r}, t)]}{\delta \rho(\mathbf{r}, t)} + V_{ext}(\mathbf{r}, t),$$

The TD charge-density:

$$\rho(\mathbf{r}, t) = \sum_i^{occ} |\varphi_i(\mathbf{r}, t)|^2.$$

The TD quantum Liouville equation:

$$[\hat{H}_{KS}(t), \hat{\rho}(t)] = i \frac{\partial}{\partial t} \hat{\rho}(t).$$

Runge and Gross, *PRL* (1984)

Onida, Reining, Rubio, *RMP* (2002)

Time-Dependent Density Functional Theory

Ground-state: DFT

The Kohn-Sham equation:

$$\left(-\frac{1}{2}\nabla^2 + V_{KS}(\mathbf{r})\right) \varphi_i(\mathbf{r}) = \varepsilon_i \varphi_i(\mathbf{r}).$$

The Kohn-Sham potential $V_{KS}(\mathbf{r})$:

$$\int \frac{\rho(\mathbf{r}')}{|\mathbf{r}-\mathbf{r}'|} d\mathbf{r}' + \frac{\delta E_{xc}[\rho(\mathbf{r})]}{\delta \rho(\mathbf{r})} + V_{ext}(\mathbf{r}).$$

The charge-density:

$$\rho(\mathbf{r}) = \sum_i^{occ} |\varphi_i(\mathbf{r})|^2.$$

The quantum Liouville equation:

$$[\hat{H}_{KS}, \hat{\rho}] = 0.$$

Hohenberg and Kohn, *Phys. Rev.* (1964)

Kohn and Sham, *Phys. Rev.* (1965)

Excited-state: TDDFT

The TD Kohn-Sham equation:

$$\left(-\frac{1}{2}\nabla^2 + V_{KS}(\mathbf{r}, t)\right) \varphi_i(\mathbf{r}, t) = i \frac{\partial}{\partial t} \varphi_i(\mathbf{r}, t).$$

The TD Kohn-Sham potential $V_{KS}(\mathbf{r}, t)$:

$$\int \frac{\rho(\mathbf{r}', t)}{|\mathbf{r}-\mathbf{r}'|} d\mathbf{r}' + \frac{\delta E_{xc}[\rho(\mathbf{r}, t)]}{\delta \rho(\mathbf{r}, t)} + V_{ext}(\mathbf{r}, t),$$

The TD charge-density:

$$\rho(\mathbf{r}, t) = \sum_i^{occ} |\varphi_i(\mathbf{r}, t)|^2.$$

The TD quantum Liouville equation:

$$[\hat{H}_{KS}(t), \hat{\rho}(t)] = i \frac{\partial}{\partial t} \hat{\rho}(t).$$

Runge and Gross, *PRL* (1984)

Onida, Reining, Rubio, *RMP* (2002)

Fluctuation-dissipation theorem

Optical absorption

Perturbation: electric field



Polarization of the dipole:

$$\mathbf{d}(\omega) = \chi(\omega) \mathbf{E}_{\text{ext}}(\omega)$$

χ is the polarization-polarization correlation function

$$\text{Im } \epsilon(\omega) \propto S(\omega)$$

$$S(\omega) = \frac{2}{\pi} \omega \text{Im } \chi(\omega)$$

S is the oscillator strength

- ▶ $\text{Im } \epsilon$: Measured experimentally
- ▶ S : Fluctuation of polarization
- ▶ $\text{Im } \chi$: Dissipation of energy

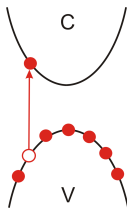
Two implementations of linear-response TDDFPT

Optical absorption spectra of finite systems

Conventional TDDFT approach

Independent-transition polarizability χ^0

$$\chi^0(\omega) = \sum_{v,c} (f_v - f_c) \frac{\varphi_c(\mathbf{r}) \varphi_v^*(\mathbf{r}) \varphi_v(\mathbf{r}') \varphi_c(\mathbf{r}')}{\omega - (\epsilon_c - \epsilon_v) + i\eta}$$



Dyson-like equation:

$$\chi = \chi^0 + \chi^0 (v_{Coul} + f_{xc}) \chi$$

Onida, Reining, Rubio, RMP (2002)

Liouville-Lanczos approach

Definition:

$$\chi(\omega) \equiv \text{Tr} \left(\tilde{V}'_{ext}(\mathbf{r}, \omega) \hat{\rho}'(\omega) \right)$$

$$\hat{\rho}'(\omega) = ?$$

Quantum Liouville equation:

$$[\hat{H}_{KS}(t), \hat{\rho}(t)] = i \frac{\partial}{\partial t} \hat{\rho}(t)$$

Linearization + Fourier transform:

$$(\omega - \hat{L}) \cdot \hat{\rho}'(\omega) = [\tilde{V}'_{ext}(\omega), \hat{\rho}^0]$$

$$\hat{L} \cdot \hat{\rho}' \equiv [\hat{H}_{KS}^0, \hat{\rho}'] + [\hat{V}_{HXC}, \hat{\rho}^0]$$

$$\chi(\omega) = \langle \tilde{V}'_{ext}(\omega) | (\omega - \hat{L})^{-1} [\tilde{V}'_{ext}(\omega), \hat{\rho}^0] \rangle$$



Use of Lanczos recursion method

Rocca, Gebauer, Saad, Baroni, JCP (2008)

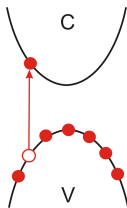
Two implementations of linear-response TDDFPT

Optical absorption spectra of finite systems

Conventional TDDFT approach

Independent-transition polarizability χ^0

$$\chi^0(\omega) = \sum_{v,c} (f_v - f_c) \frac{\varphi_c(\mathbf{r}) \varphi_v^*(\mathbf{r}) \varphi_v(\mathbf{r}') \varphi_c(\mathbf{r}')}{\omega - (\epsilon_c - \epsilon_v) + i\eta}$$



Dyson-like equation:

$$\chi = \chi^0 + \chi^0 (v_{Coul} + f_{xc}) \chi$$

Onida, Reining, Rubio, RMP (2002)

Liouville-Lanczos approach

Definition:

$$\chi(\omega) \equiv \text{Tr} \left(\tilde{V}'_{ext}(\mathbf{r}, \omega) \hat{\rho}'(\omega) \right)$$

$$\hat{\rho}'(\omega) = ?$$

Quantum Liouville equation:

$$[\hat{H}_{KS}(t), \hat{\rho}(t)] = i \frac{\partial}{\partial t} \hat{\rho}(t)$$

Linearization + Fourier transform:

$$(\omega - \hat{L}) \cdot \hat{\rho}'(\omega) = [\tilde{V}'_{ext}(\omega), \hat{\rho}^0]$$

$$\hat{L} \cdot \hat{\rho}' \equiv [\hat{H}_{KS}^0, \hat{\rho}'] + [\hat{V}_{HXC}, \hat{\rho}^0]$$

$$\chi(\omega) = \langle \tilde{V}'_{ext}(\omega) | (\omega - \hat{L})^{-1} [\tilde{V}'_{ext}(\omega), \hat{\rho}^0] \rangle$$



Use of Lanczos recursion method

Rocca, Gebauer, Saad, Baroni, JCP (2008)

Outline

1. Introduction

1.1 Motivation

1.2 Material: Bismuth

1.3 State of the art methods

2. Results

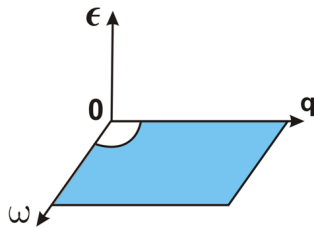
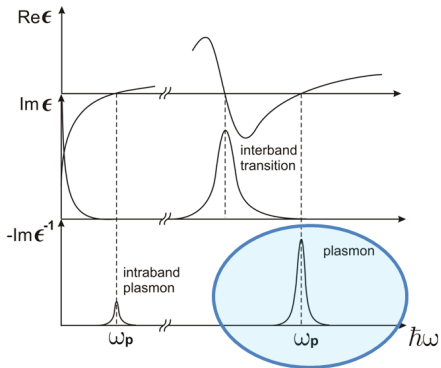
2.1 High-energy response: new approach for EELS

2.2 Low-energy response: free-carrier response

3. Conclusions

High-energy response

EELS: $\mathbf{q} \neq 0, \omega \neq 0$



Fluctuation-dissipation theorem

Optical absorption

Perturbation: electric field



Polarization of the dipole:

$$\mathbf{d}(\omega) = \chi(\omega) \mathbf{E}_{\text{ext}}(\omega)$$

χ is the polarization-polarization correlation function

$$\text{Im } \epsilon(\omega) \propto S(\omega)$$

$$S(\omega) = \frac{2}{\pi} \omega \text{Im } \chi(\omega)$$

S is the oscillator strength

- ▶ $\text{Im } \epsilon$: Measured experimentally
- ▶ S : Fluctuation of polarization
- ▶ $\text{Im } \chi$: Dissipation of energy

EELS

Perturbation: electron beam



Double differential cross-section:

$$\frac{d^2\sigma}{d\Omega d\omega} \propto S(\mathbf{q}, \mathbf{q}; \omega)$$

$$S(\mathbf{q}, \mathbf{q}; \omega) = -\frac{1}{\pi} \text{Im } \chi(\mathbf{q}, \mathbf{q}; \omega)$$

S is the dynamic structure factor

$\chi(\mathbf{q}, \mathbf{q}; t) = \langle\langle \hat{\rho}_{\mathbf{q}}(t) \hat{\rho}_{\mathbf{q}}(0) \rangle\rangle$ is the density-density correlation function

$$-\text{Im } \epsilon^{-1}(\mathbf{q}, \mathbf{q}; \omega) \propto -\text{Im } \chi(\mathbf{q}, \mathbf{q}; \omega)$$

- ▶ $\frac{d^2\sigma}{d\Omega d\omega}$: Measured experiment.
- ▶ S : Fluctuation of density
- ▶ $\text{Im } \chi$: Dissipation of energy

Fluctuation-dissipation theorem

Optical absorption

Perturbation: electric field



Polarization of the dipole:

$$\mathbf{d}(\omega) = \chi(\omega) \mathbf{E}_{\text{ext}}(\omega)$$

χ is the polarization-polarization correlation function

$$\text{Im } \epsilon(\omega) \propto S(\omega)$$

$$S(\omega) = \frac{2}{\pi} \omega \text{Im } \chi(\omega)$$

S is the oscillator strength

- ▶ $\text{Im } \epsilon$: Measured experimentally
- ▶ S : Fluctuation of polarization
- ▶ $\text{Im } \chi$: Dissipation of energy

EELS

Perturbation: electron beam



Double differential cross-section:

$$\frac{d^2\sigma}{d\Omega d\omega} \propto S(\mathbf{q}, \mathbf{q}; \omega)$$

$$S(\mathbf{q}, \mathbf{q}; \omega) = -\frac{1}{\pi} \text{Im } \chi(\mathbf{q}, \mathbf{q}; \omega)$$

S is the dynamic structure factor

$\chi(\mathbf{q}, \mathbf{q}; t) = \langle\langle \hat{\rho}_{\mathbf{q}}(t) \hat{\rho}_{\mathbf{q}}(0) \rangle\rangle$ is the density-density correlation function

$$-\text{Im } \epsilon^{-1}(\mathbf{q}, \mathbf{q}; \omega) \propto -\text{Im } \chi(\mathbf{q}, \mathbf{q}; \omega)$$

- ▶ $\frac{d^2\sigma}{d\Omega d\omega}$: Measured experiment.
- ▶ S : Fluctuation of density
- ▶ $\text{Im } \chi$: Dissipation of energy

TDDFPT: Liouville-Lanczos approach

Optical absorption

Perturbation: electric field

Definition:

$$\chi(\omega) \equiv \text{Tr} \left(\tilde{V}'_{\text{ext}}(\mathbf{r}, \omega) \hat{\rho}'(\omega) \right)$$

$$\hat{\rho}'(\omega) = ?$$

Quantum Liouville equation:

$$[\hat{H}_{KS}(t), \hat{\rho}(t)] = i \frac{\partial}{\partial t} \hat{\rho}(t)$$

Linearization + Fourier transformation:

$$(\omega - \hat{L}) \cdot \hat{\rho}'(\omega) = [\tilde{V}'_{\text{ext}}(\omega), \hat{\rho}^0]$$

$$\hat{L} \cdot \hat{\rho}' \equiv [\hat{H}_{KS}^0, \hat{\rho}'] + [\hat{V}_{\text{HXC}}, \hat{\rho}^0]$$

$$\chi(\omega) = \langle \tilde{V}'_{\text{ext}}(\omega) | (\omega - \hat{L})^{-1} [\tilde{V}'_{\text{ext}}(\omega), \hat{\rho}^0] \rangle$$



Use of Lanczos recursion method

EELS

Perturbation: electron beam

Definition:

$$\chi(\mathbf{q}, \mathbf{q}; \omega) \equiv \text{Tr} \left(\tilde{V}'_{\text{ext}, \mathbf{q}}(\mathbf{r}, \omega) \hat{\rho}'_{\mathbf{q}}(\omega) \right)$$

$$\hat{\rho}'_{\mathbf{q}}(\omega) = ?$$

Quantum Liouville equation:

$$[\hat{H}_{KS}(t), \hat{\rho}_{\mathbf{q}}(t)] = i \frac{\partial}{\partial t} \hat{\rho}_{\mathbf{q}}(t)$$

Linearization + Fourier transformation:

$$(\omega - \hat{L}) \cdot \hat{\rho}'_{\mathbf{q}}(\omega) = [\tilde{V}'_{\text{ext}, \mathbf{q}}(\omega), \hat{\rho}^0]$$

$$\hat{L} \cdot \hat{\rho}'_{\mathbf{q}} \equiv [\hat{H}_{KS}^0, \hat{\rho}'_{\mathbf{q}}] + [\hat{V}_{\text{HXC}, \mathbf{q}}, \hat{\rho}^0]$$

$$\chi(\mathbf{q}, \mathbf{q}; \omega) = \langle \tilde{V}'_{\text{ext}, \mathbf{q}}(\omega) | (\omega - \hat{L})^{-1} [\tilde{V}'_{\text{ext}, \mathbf{q}}(\omega), \hat{\rho}^0] \rangle$$



Use of Lanczos recursion method

TDDFPT: Liouville-Lanczos approach

Optical absorption

Perturbation: electric field

Definition:

$$\chi(\omega) \equiv \text{Tr} \left(\tilde{V}'_{\text{ext}}(\mathbf{r}, \omega) \hat{\rho}'(\omega) \right)$$

$$\hat{\rho}'(\omega) = ?$$

Quantum Liouville equation:

$$[\hat{H}_{KS}(t), \hat{\rho}(t)] = i \frac{\partial}{\partial t} \hat{\rho}(t)$$

Linearization + Fourier transformation:

$$(\omega - \hat{L}) \cdot \hat{\rho}'(\omega) = [\tilde{V}'_{\text{ext}}(\omega), \hat{\rho}^0]$$

$$\hat{L} \cdot \hat{\rho}' \equiv [\hat{H}_{KS}^0, \hat{\rho}'] + [\hat{V}_{\text{HXC}}, \hat{\rho}^0]$$

$$\chi(\omega) = \langle \tilde{V}'_{\text{ext}}(\omega) | (\omega - \hat{L})^{-1} [\tilde{V}'_{\text{ext}}(\omega), \hat{\rho}^0] \rangle$$



Use of Lanczos recursion method

EELS

Perturbation: electron beam

Definition:

$$\chi(\mathbf{q}, \mathbf{q}; \omega) \equiv \text{Tr} \left(\tilde{V}'_{\text{ext}, \mathbf{q}}(\mathbf{r}, \omega) \hat{\rho}'_{\mathbf{q}}(\omega) \right)$$

$$\hat{\rho}'_{\mathbf{q}}(\omega) = ?$$

Quantum Liouville equation:

$$[\hat{H}_{KS}(t), \hat{\rho}_{\mathbf{q}}(t)] = i \frac{\partial}{\partial t} \hat{\rho}_{\mathbf{q}}(t)$$

Linearization + Fourier transformation:

$$(\omega - \hat{L}) \cdot \hat{\rho}'_{\mathbf{q}}(\omega) = [\tilde{V}'_{\text{ext}, \mathbf{q}}(\omega), \hat{\rho}^0]$$

$$\hat{L} \cdot \hat{\rho}'_{\mathbf{q}} \equiv [\hat{H}_{KS}^0, \hat{\rho}'_{\mathbf{q}}] + [\hat{V}_{\text{HXC}, \mathbf{q}}, \hat{\rho}^0]$$

$$\chi(\mathbf{q}, \mathbf{q}; \omega) = \langle \tilde{V}'_{\text{ext}, \mathbf{q}}(\omega) | (\omega - \hat{L})^{-1} [\tilde{V}'_{\text{ext}, \mathbf{q}}(\omega), \hat{\rho}^0] \rangle$$



Use of Lanczos recursion method

Pros & Contras

Conventional TDDFT approach

☹ Numerous empty states

$$\chi^0(\omega) = \sum_{v,c} (f_v - f_c) \frac{\varphi_c(\mathbf{r}) \varphi_v^*(\mathbf{r}) \varphi_v(\mathbf{r}') \varphi_c(\mathbf{r}')}{\omega - (\varepsilon_c - \varepsilon_v) + i\eta}$$

☹ Multiplication and inversion of large matrices

$$\chi = \chi^0 + \chi^0 (v_{Coul} + f_{xc}) \chi$$

☹ Calculation of χ^0 and χ must be repeated for each frequency

☹ **Scaling:**

$$[N_v \times N_c \times N_k \times N_G^2 + N_G^{2.4}] \times N_\omega$$

☺ Approximations beyond the adiabatic one are possible: $f_{xc}(\omega)$

Liouville-Lanczos approach

☺ No empty states (use of DFPT techniques)

☺ No matrix inversions (use of Lanczos recursion method)

☺ Lanczos recursion has to be done **once** for all frequencies

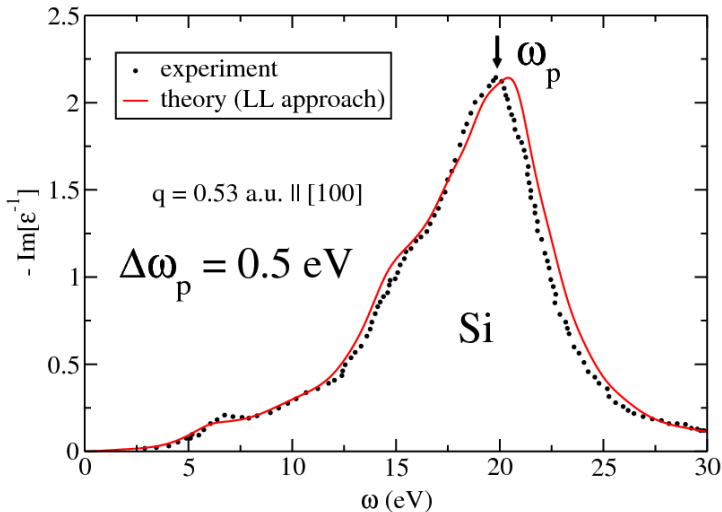
☺ **Scaling:** Only a few times larger than ground-state DFT calculations:

$$\alpha [N_v \times N_k \times N_{PW} \ln N_{PW}] \times N_{iter}$$

☹ Limitation by the adiabatic approximation: static f_{xc}

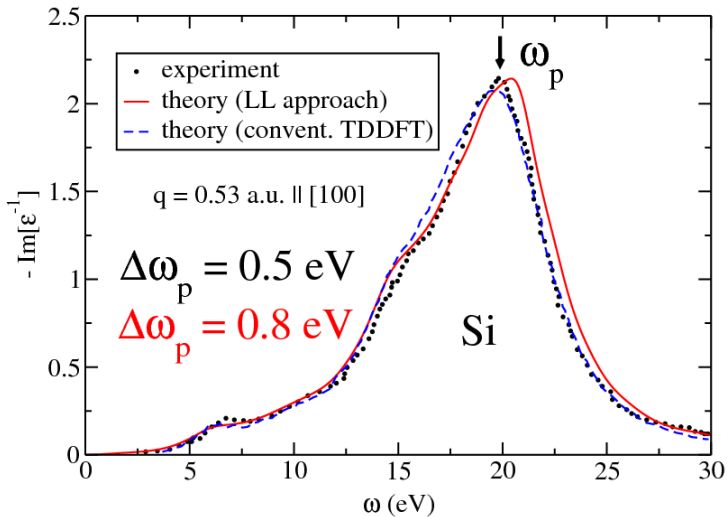
Testing of the Liouville-Lanczos approach

Plasmon peak position } agree with $\left\{ \begin{array}{l} \text{experiment} \\ \text{conventional TDDFT approach} \end{array} \right.$
Integrated intensity



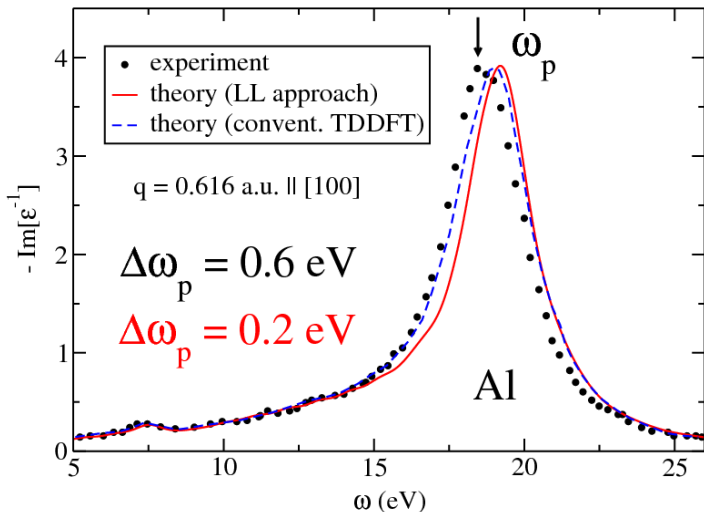
Testing of the Liouville-Lanczos approach

Plasmon peak position } agree with $\left\{ \begin{array}{l} \text{experiment} \\ \text{conventional TDDFT approach} \end{array} \right.$
Integrated intensity



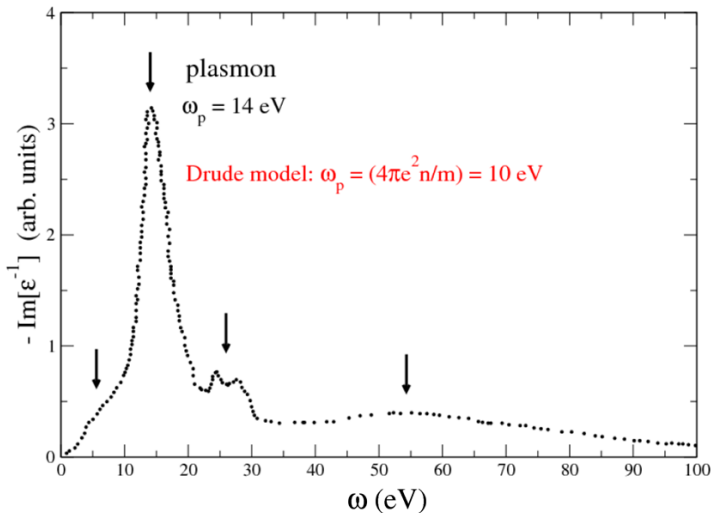
Testing of the Liouville-Lanczos approach

Plasmon peak position } agree with $\left\{ \begin{array}{l} \text{experiment} \\ \text{conventional TDDFT approach} \end{array} \right.$
Integrated intensity



Experimental EEL spectrum of Bi for $q \rightarrow 0$

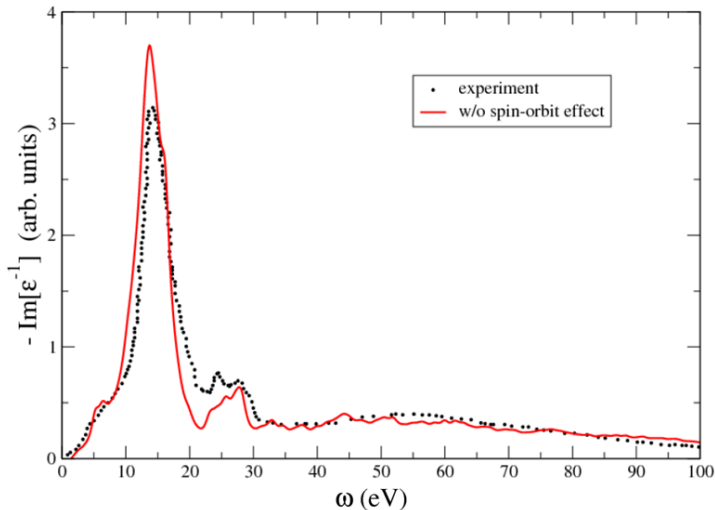
Ab initio calculations are needed to understand the origin of 4 features.



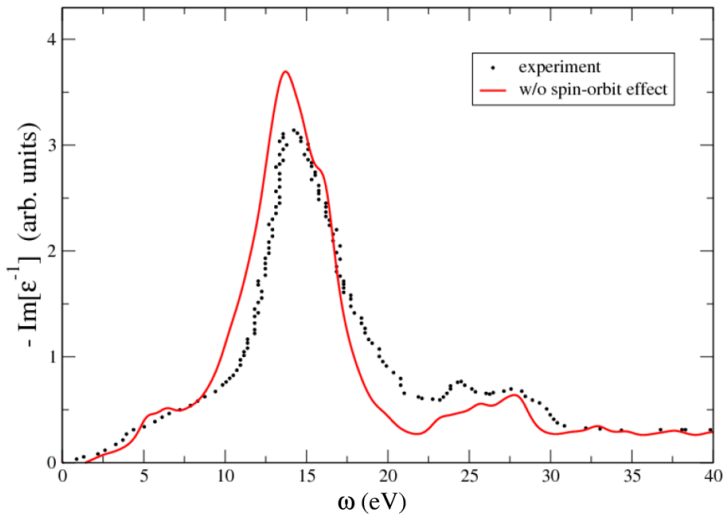
C. Wehenkel et al., *Solid State Comm.* **15**, 555 (1974)

Comparison between experiment and theory

- ▶ Four features in the EEL spectrum are well reproduced.
- ▶ Accurate description of the the broad structure in 40 - 100 eV range.

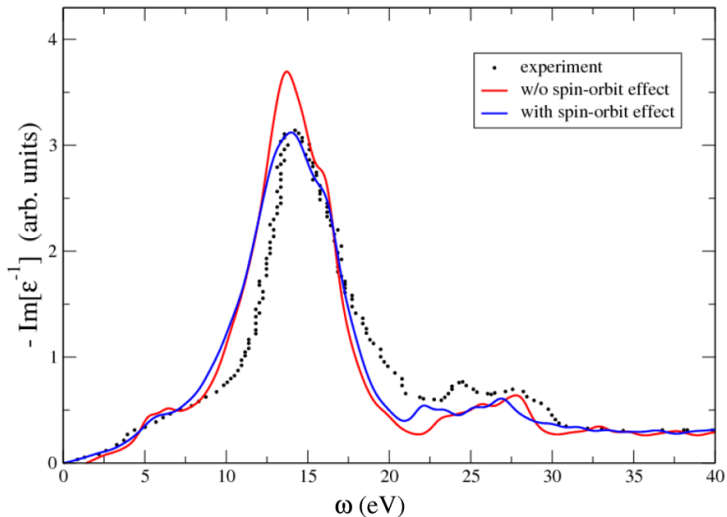


Effect of the spin-orbit coupling (SOC)



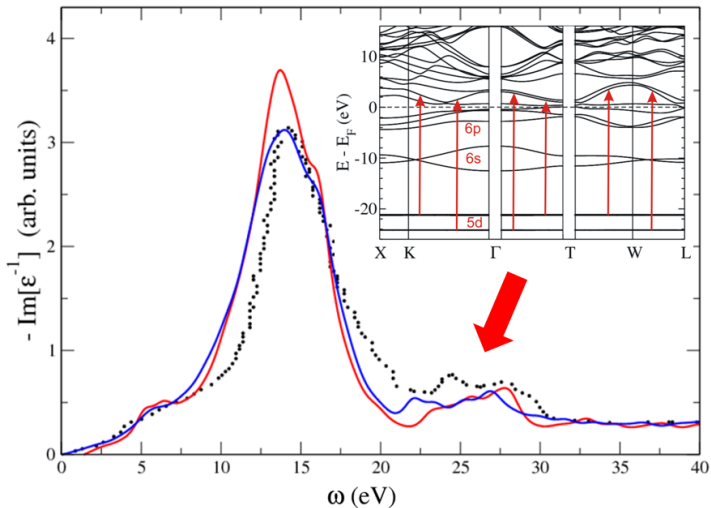
Effect of the spin-orbit coupling (SOC)

- ▶ Integrated intensity is improved by SOC.
- ▶ Red-shift of peaks in the range 20 - 30 eV, due to splitting of 5d levels.



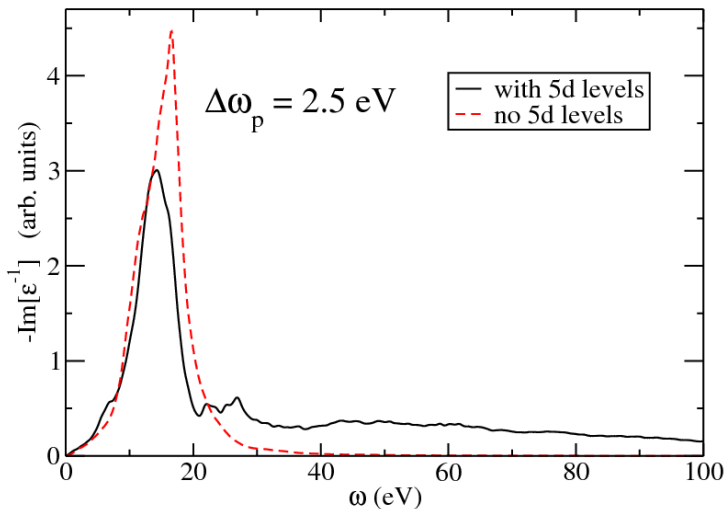
Origin of the peaks between 20 - 30 eV

Interband transitions from the 5d semicore levels to lowest unoccupied levels.



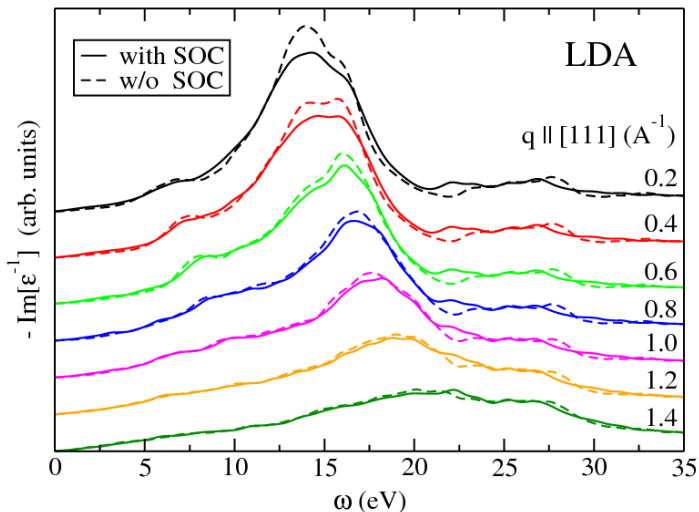
Effect of the 5d semicore levels

Ionization from 5d semicore levels \implies broad structure between 40 - 100 eV.

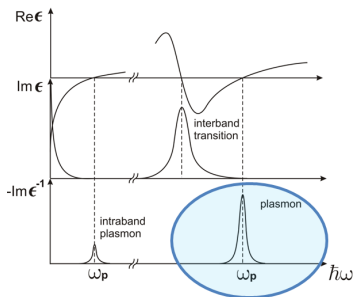


Plasmon dispersion

- ▶ Increase of $q \Rightarrow$ blue-shift of the plasmon peak.
- ▶ Plasmon enters in electron-hole continuum \Rightarrow broadening of spectrum.



Conclusions (I)



- ▶ Developed a **new method for EELS** - Liouville-Lanczos approach;
- ▶ The new method is computationally **more efficient** than conventional TDDFT method;
- ▶ The new method tested **successfully** on bulk Si and Al;
- ▶ **First *ab initio* calculations** of the EEL spectra in bulk Bi.

Outline

1. Introduction

1.1 Motivation

1.2 Material: Bismuth

1.3 State of the art methods

2. Results

2.1 High-energy response: new approach for EELS

2.2 Low-energy response: free-carrier response

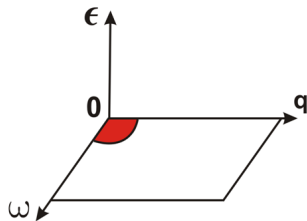
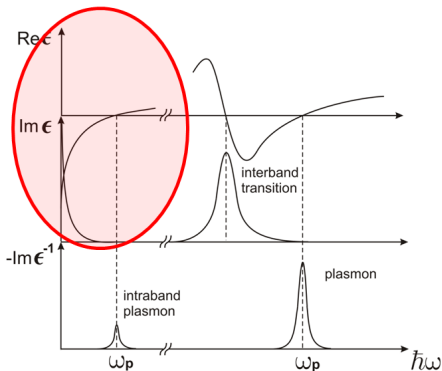
3. Conclusions

Low-energy response

Optics: $\mathbf{q} \rightarrow 0, \omega \rightarrow 0$

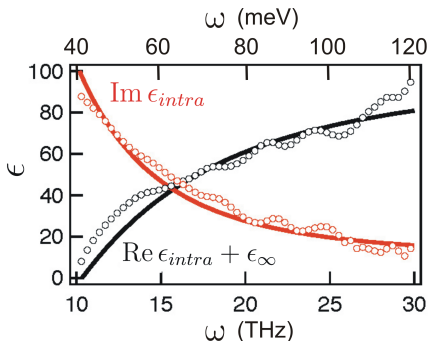
Drude intraband contribution to the dielectric function:

$$\epsilon_{intra}(\omega) = 1 - \frac{\omega_p^2}{\omega(\omega + i\gamma)}$$



Dielectric properties of Bi in equilibrium: Free carrier response

Time-resolved (pump-probe) terahertz experiment: L. Perfetti, J. Faure, T. Kampfrath, C. R. Ast, C. Frischkorn, M. Wolf.



Circles: Experimental data

Solid lines: Fit by Drude model

The Drude model accurately fits expt. data \implies Free carrier response

Drude model:

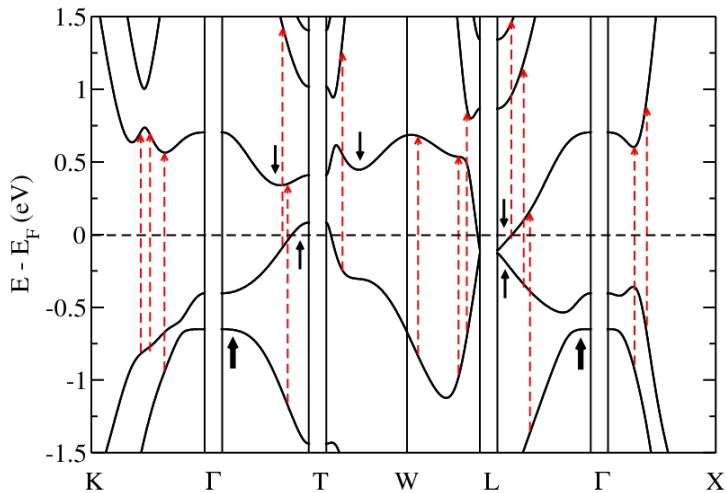
$$\epsilon(\omega) = -\frac{\omega_{p,\text{eq}}^2}{\omega(\omega + i\gamma)} + \epsilon_{\infty}$$

\Downarrow

Fitting:

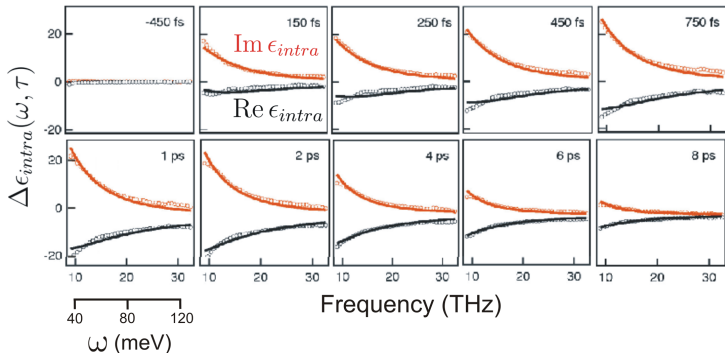
Plasma freq. $\omega_{p,\text{eq}} = 560$ meV,
Scattering rate $\gamma = 37$ meV,
and $\epsilon_{\infty} = 100$.

Photoexcited bismuth ($\mathbf{q} = 0$, $\hbar\omega = 1.6$ eV)



Photoexcited bismuth ($\mathbf{q} = 0$, $\hbar\omega = 1.6$ eV)

$\Delta\epsilon_{intra}(\omega)$ is the change of the intraband dielectric function due to the photoexcitation of bismuth.

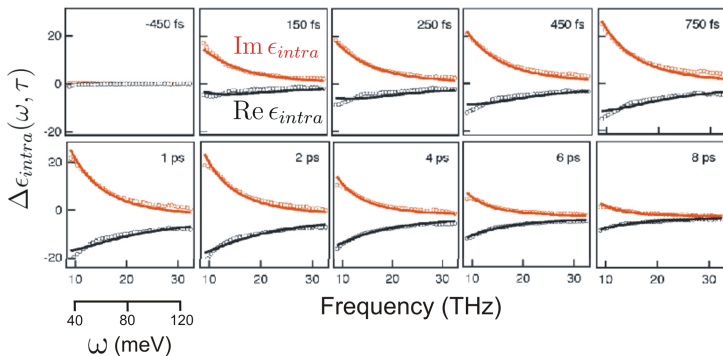


$\Delta\epsilon_{intra}(\omega)$ displays a **free carrier response**.

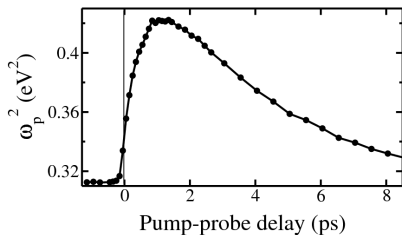
Fitting by the **Drude model**:

$$\Delta\epsilon_{intra}(\omega) = 1 - \frac{\Delta\omega_p^2}{\omega(\omega + i\gamma)}, \quad \omega_p^2 = \omega_{p,eq}^2 + \Delta\omega_p^2.$$

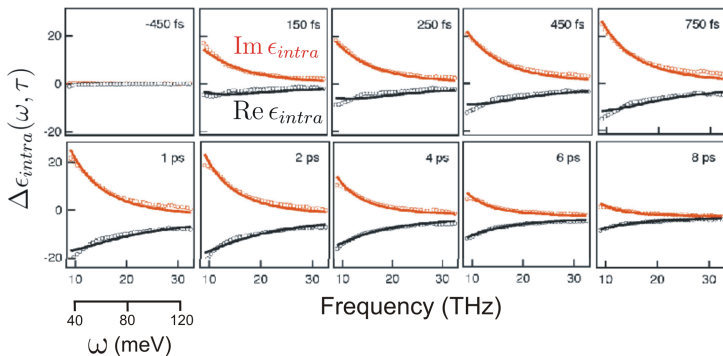
Photoexcited bismuth ($\mathbf{q} = 0$, $\hbar\omega = 1.6$ eV)



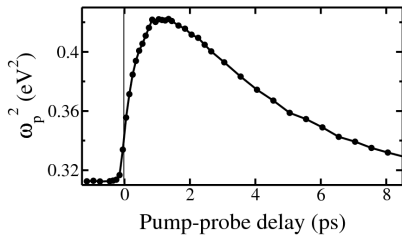
BISMUTH



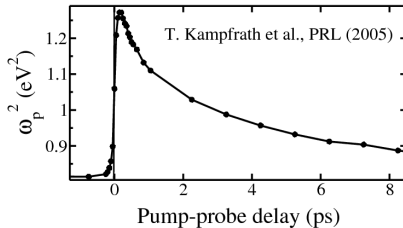
Photoexcited bismuth ($\mathbf{q} = 0$, $\hbar\omega = 1.6$ eV)



BISMUTH

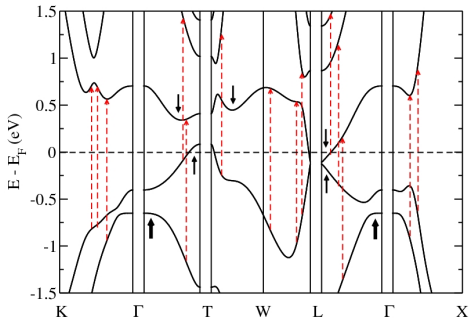


GRAPHITE



Hypothesis

Just after the photoexcitation, electrons and holes stick in the true local extrema of the valence and conduction bands.



Drude model:

$$\Delta\omega_p^2 = \frac{4\pi e^2 \Delta n}{m}$$

$$\uparrow \Delta n \implies \uparrow \Delta\omega_p^2$$

Effective mass approximation
for the true local extrema:

$$\left[m^{*-1}(\mathbf{k}) \right]_{ij} = \frac{1}{\hbar^2} \frac{\partial^2 E(\mathbf{k})}{\partial k_i \partial k_j}$$

Verification of the hypothesis: compare average effective masses of the true local extrema with optical masses near the T and L points.

Optical mass at L and T points

Definition of the **optical mass** on the basis of the Drude model:

$$\Delta\omega_p^2(T) = \frac{4\pi e^2 \Delta n(T)}{m^{op}}$$

Semiclassical model:

$$\Delta\omega_p^2(T) = \frac{4\pi e^2}{3} v_F^2 \int g(E) [f'_{FD}(E, T_0) - f'_{FD}(E, T)] dE$$

$$\Delta n(T) = \int g(E) |f_{FD}(E, T) - f_{FD}(E, T_0)| dE$$

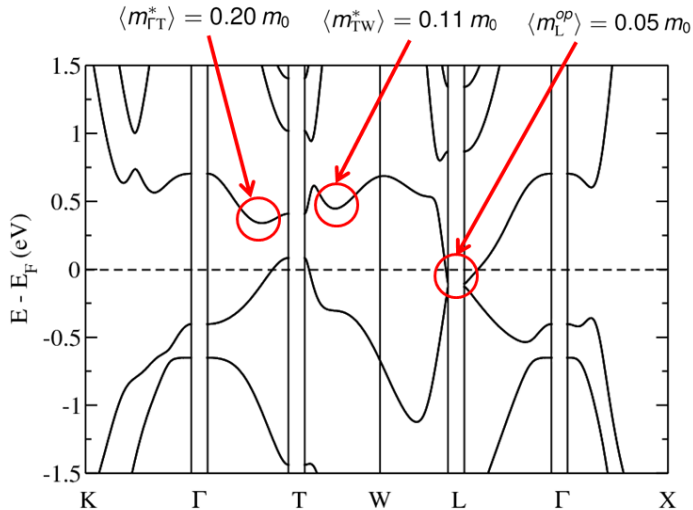
where $g(E)$ is the restricted DOS,

v_F is the Fermi velocity of carriers,

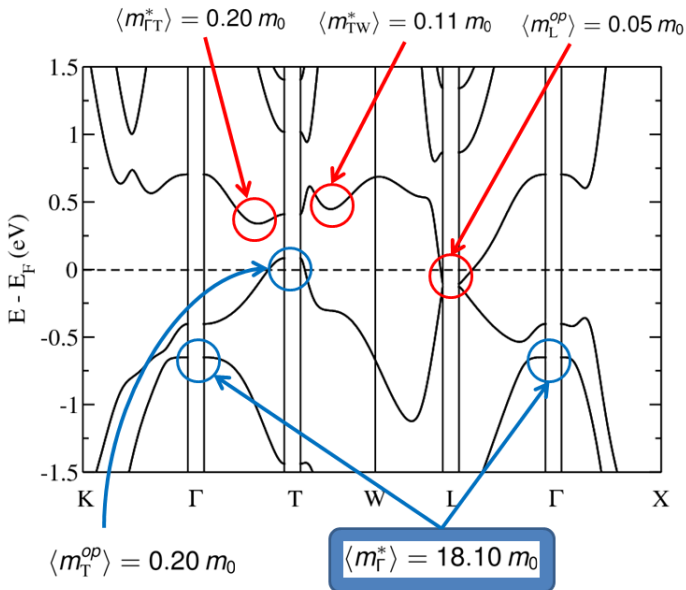
f_{FD} is the Fermi-Dirac distribution function.

$g(E)$ and v_F were calculated from first principles.

Photoexcited electrons and holes get stuck in true local extrema

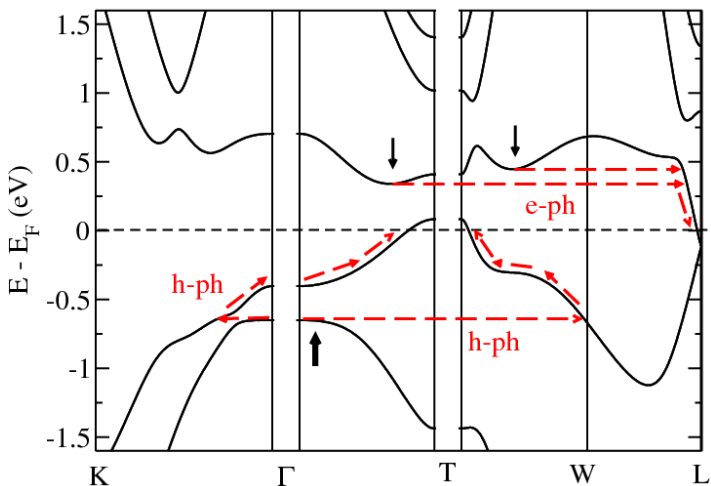


Photoexcited electrons and holes get stuck in true local extrema



Relaxation of carriers

The relaxation of carriers occurs due to electron-phonon (e-ph) and hole-phonon (h-ph) scattering, and Auger recombination.

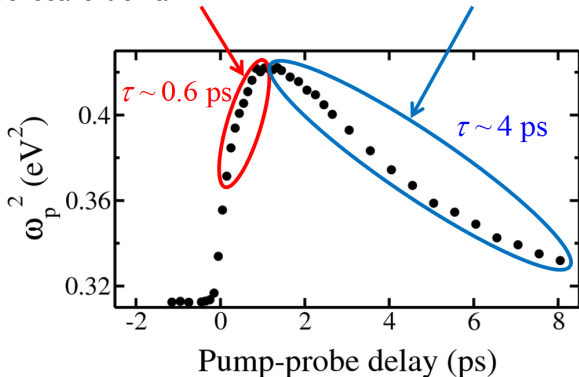


Two regimes in the evolution of the plasma frequency

Rate equations \implies relaxation times τ

Relaxation of electrons and holes, which were stuck in the true local extrema

Electron-hole recombination near the Fermi level



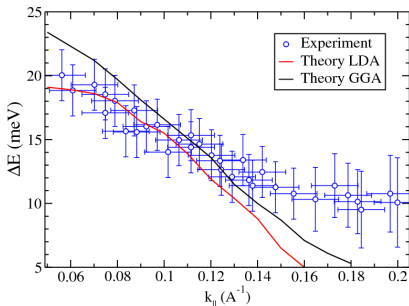
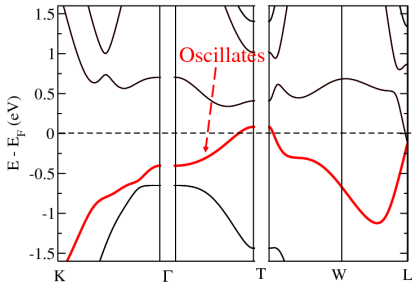
Ab initio calculation of electron-phonon coupling

Photoemission experiment: L. Perfetti and J. Faure

At higher fluence of the photoexcitation (0.6 mJ/cm^2), the A_{1g} phonon mode is activated in bismuth.

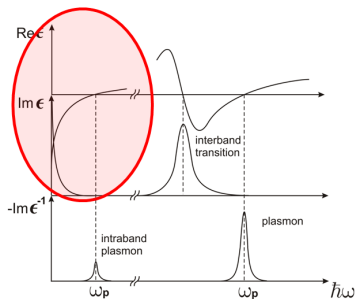


Due to **electron-phonon interaction**, the highest valence bulk band oscillates with the frequency of the A_{1g} phonon mode.



E. Papalazarou, I. Timrov, N. Vast, L. Perfetti et al., PRL 108, 256808 (2012).

Conclusions (II)



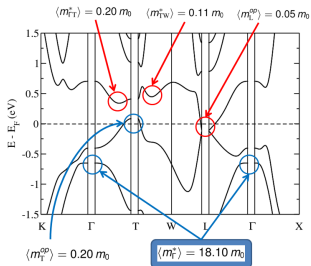
- ▶ Theoretical description of free carrier response in photoexcited Bi.
- ▶ Evolution of the plasma frequency displays two regimes due to the existence of true local extrema in the band structure of Bi.
- ▶ Relaxation of carriers occurs with a time rate of 0.6 ps, and the electron-hole recombination occurs with a time rate of 4 ps.
- ▶ Wavevector-dependence of electron-phonon coupling is in agreement with experiment.

General conclusions (I)

1. Description of the full charge-carrier response in excited bismuth from low energy to high energy range.

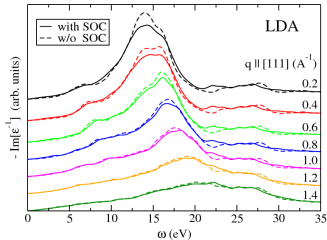
Low-energy response:

Theoretical model for the description of the free carrier dynamics in photoexcited bismuth.



High-energy response:

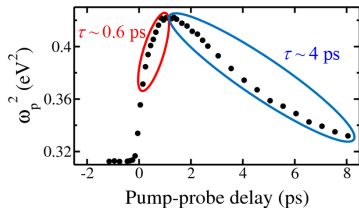
New method for EELS and application to bismuth.



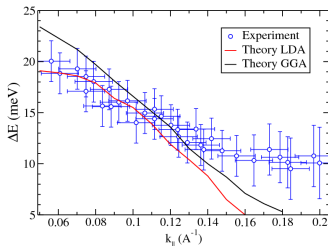
General conclusions (II)

2. Importance of the electron-phonon coupling for the interpretation of photoexcited bismuth.

Relaxation times in photoexcited bismuth: 0.6 ps for carrier-phonon scattering, and 4 ps for electron-phonon recombination.



Ab initio calculations of wave-vector-dependent electron-phonon coupling are in good agreement with experiment.



Perspectives

- ▶ Spin-orbit coupling: from bulk to surfaces
 - ▶ Surfaces of Bi and of Bi compounds (Bi_2Te_3 , Bi_2Se_3)
- ▶ Importance of electron-phonon coupling
 - ▶ Relaxation times in Bi
 - ▶ Thermoelectricity in Bi and Bi compounds (Bi_2Te_3 , Bi_2Se_3)
 - ▶ Occurrence of charge density waves in some materials
- ▶ Application of the Liouville-Lanczos approach for large systems
 - ▶ Surface plasmons
 - ▶ Acoustic surface plasmons

Collaborations

Laboratoire des Solides Irradiés, École Polytechnique

Nathalie Vast, Luca Perfetti, Jelena Sjakste, Jérôme Faure, Paola Gava

SISSA – Scuola Internazionale Superiore di Studi Avanzati

Stefano Baroni

ICTP – The Abdus Salam International Centre for Theoretical Physics

Ralph Gebauer

Perspectives

- ▶ Spin-orbit coupling: from bulk to surfaces
 - ▶ Surfaces of Bi and of Bi compounds (Bi_2Te_3 , Bi_2Se_3)
- ▶ Importance of electron-phonon coupling
 - ▶ Relaxation times in Bi
 - ▶ Thermoelectricity in Bi and Bi compounds (Bi_2Te_3 , Bi_2Se_3)
 - ▶ Occurrence of charge density waves in some materials
- ▶ Application of the Liouville-Lanczos approach for large systems
 - ▶ Surface plasmons
 - ▶ Acoustic surface plasmons